Journal of
Nanoscience and Nanotechnology
Vol. 8, 1–5, 2008

Fabrication of Gold Nanotubes from Removable MgO Nanowires Templates

Hyoun Woo Kim*, Jong Woo Lee, Mesfin A. Kebede,
Hyo Sung Kim, Buddhudu Srinivasa, and Chongmu Lee

School of Materials Science and Engineering, Inha University, Incheon 402-751, Republic of Korea

We have prepared MgO/Au core–shell nanowires, subsequently demonstrating the fabrication of Au nanotubes by using MgO nanowires as a sacrificial template. The samples were characterized by scanning electron microscopy, X-ray diffraction, transmission electron microscopy, and energy-dispersive X-ray spectroscopy. MgO nanowires were coated with a conformal layer of Au via sputtering. By etching away the MgO core in aqueous $(NH_3)_2SO_4$ solution, hollow nanotube-like structures of Au were readily obtained. This approach offers a potentially useful route for the fabrication of a variety of hollow metallic structures.

Keywords: Gold Nanotubes, MgO Nanowires, Templates.

1. INTRODUCTION

Gold (Au) nanostructures have found applications in biological probes,[1] submicrometer metallic barcodes,[2] surface-enhanced Raman spectroscopy,[3,4] plasmon waveguides for optical devices,[5] photonic materials,[6] and chemical sensors.[7] Also, there is currently growing interest in the fabrication of one-dimensional (1D) materials. One particularly interesting area of 1D nanostructure research is core–shell composite nanostructures known as Au nanotubes, which have a central nonmetal or hollow core surrounded by an Au wall. Au nanotubes have been used in various applications, such as molecular sieves,[8,9] sensors,[10] conductors,[11] a liftoff mask in advanced lithography,[12] catalysts for oxidation of CO,[13] and label-free quantification of DNA sequences.[14] Accordingly, they have been synthesized by a variety of techniques, including irradiation of an Au film with an electron beam at 150 K[15] and via the use of template-based electroless plating techniques, where Au is deposited onto the pore walls of a porous polymetric membrane.[16–18]

In the present study, we suggest a new synthetic approach where sputtering is used to coat a thin Au shell onto as-synthesized MgO nanowires. MgO nanowires are easy to prepare and are suitable for the use of sacrificial templates. Also, MgO is an important material for such applications as catalysis, superconductor products, and oproelectronics.[19–21] The MgO nanowires were removed by dipping them in a dilute $(NH_3)_2SO_4$ solution to obtain hollow Au nanotubes. This simple and low-cost dipping method in conjunction with an easily controlled sputtering technique presents exciting prospects for the commercial production of metal nanotubes with a variety of applications.

2. EXPERIMENTAL DETAILS

A multi-step process was used to fabricate Au nanotubes. First, pure MgB_2 powders and Au-coated substrates were placed on the lower and upper holder, respectively, in the middle of a quartz tube. The apparatus used in this study has been illustrated elsewhere.[22] The system consists of a quartz-tube reactor that is inserted into a horizontal tube furnace. During the experiment, the furnace was maintained at a temperature of 900 °C for 1 h. The typical percentage of O_2 partial pressure was set to approximately 3%, with the O_2 gas in a balance of argon being at a constant total pressure of 2 Torr.

Second, we carried out coating experiments on the as-prepared MgO nanowires using a turbo sputter coater (Emitech K575X, Emitech Ltd., Ashford, Kent, UK). The sputtering target used in the present experiment was a piece of polished *p*-type (100) Si wafer, with the distance between the target and nanowires being about 50 mm. The sputtering deposition was carried out at a pressure of 8×10^{-4} Pa in high purity argon (Ar) gas (99.999%) with a DC sputtering current of 30 mA, at room temperature. For variation of the thickness of the Au shell layer, the sputter time was set to 1 min and 3 min, respectively. Subsequently, in order to selectively remove the MgO core

*Author to whom correspondence should be addressed.

RESEARCH ARTICLE

from the MgO-Au core–shell nanowires, the sample was dipped into an aqueous $(NH_3)_2SO_4$ solution (3%) at 80 °C for 20 min. The Au shell is inert to the solvent, whereas the MgO core dissolves.

The morphology, chemical composition, and structure of the products were characterized by glancing angle (0.5°) X-ray diffraction (XRD, X'pert MPD-Philips with Cu$K\alpha_1$ radiation) with the contribution from the substrate minimized, scanning electron microscopy (SEM, Hitachi S-4200), and transmission electron microscopy (TEM, Philips CM-200). The Philips CM-200 TEM was equipped with an energy-dispersive X-ray (EDX) spectrometer. TEM samples were prepared by ultrasonically dispersing the product in acetone, and a drop of the dispersion solution was then placed on a porous carbon (Cu) film supported on a copper (Cu) microgrid.

3. RESULTS AND DISCUSSION

Figures 1(a), (b), and (c) show typical top-view SEM images of the core (MgO) structures and the core/shell structures sputtered for 1 min and 3 min, respectively. The surface of the Au shell layers is relatively smooth, and thus it is evident that the 1D-morphology of the products has not been changed by the coating process. Accordingly, we suggest that the present sputtering process is associated with a layer (Frank-van der Merwe) growth mode. Figures 2(a), (b), and (c) display XRD patterns of core (MgO) structures and core/shell structures sputtered for 1 min and 3 min, respectively. In Figures 2(b and c), all the diffraction peaks can be indexed to cubic MgO with

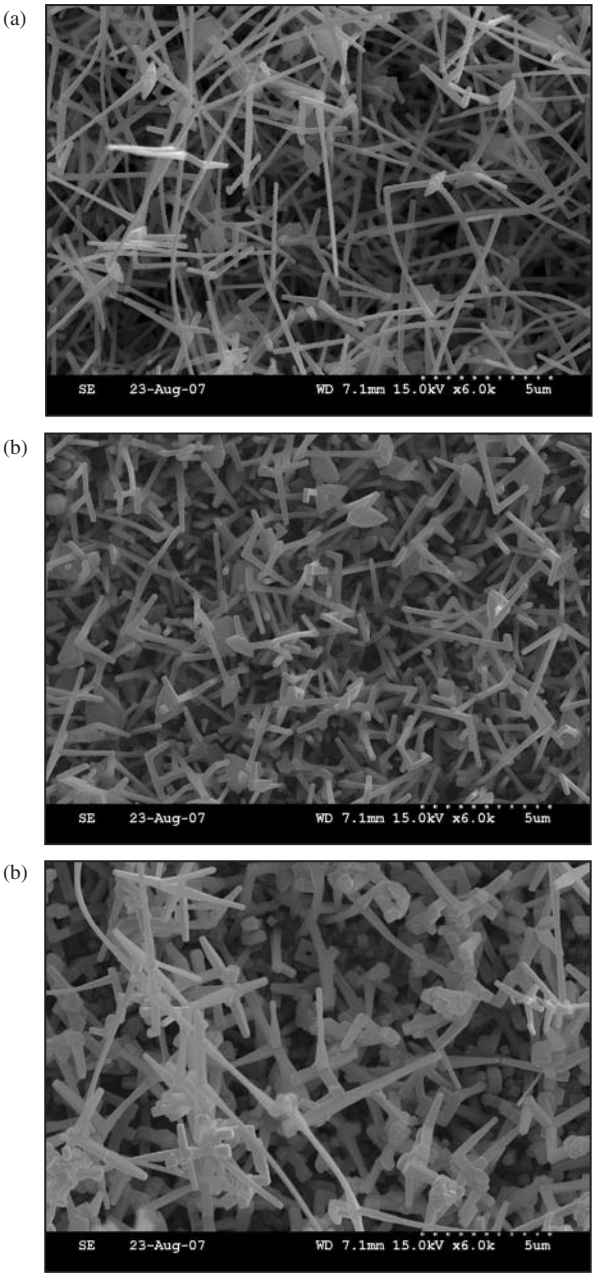

Fig. 1. SEM images of (a) core (MgO) structures and core/shell structures sputtered for (b) 1 min and (c) 3 min, respectively.

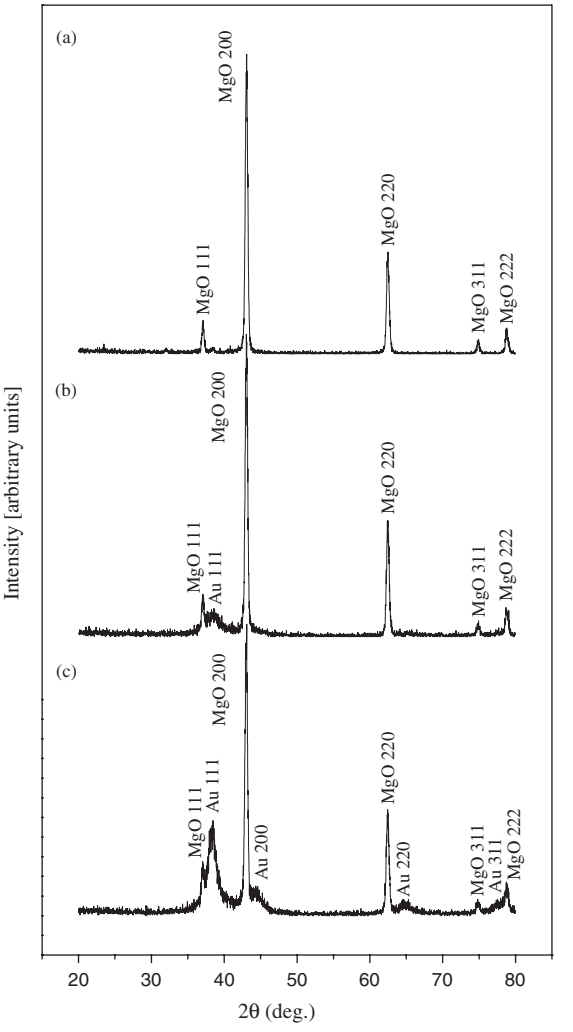

Fig. 2. XRD patterns of (a) core (MgO) structures and core/shell structures sputtered for (b) 1 min and (c) 3 min, respectively.

RESEARCH ARTICLE

a lattice constant comparable to the value of JCPDS 04-0829 or a cubic Au structure with a lattice constant $a = 0.408$ nm (JCPDS: 04-0784), whereas Figure 2(a) shows that the core structure is mainly composed of MgO phase.

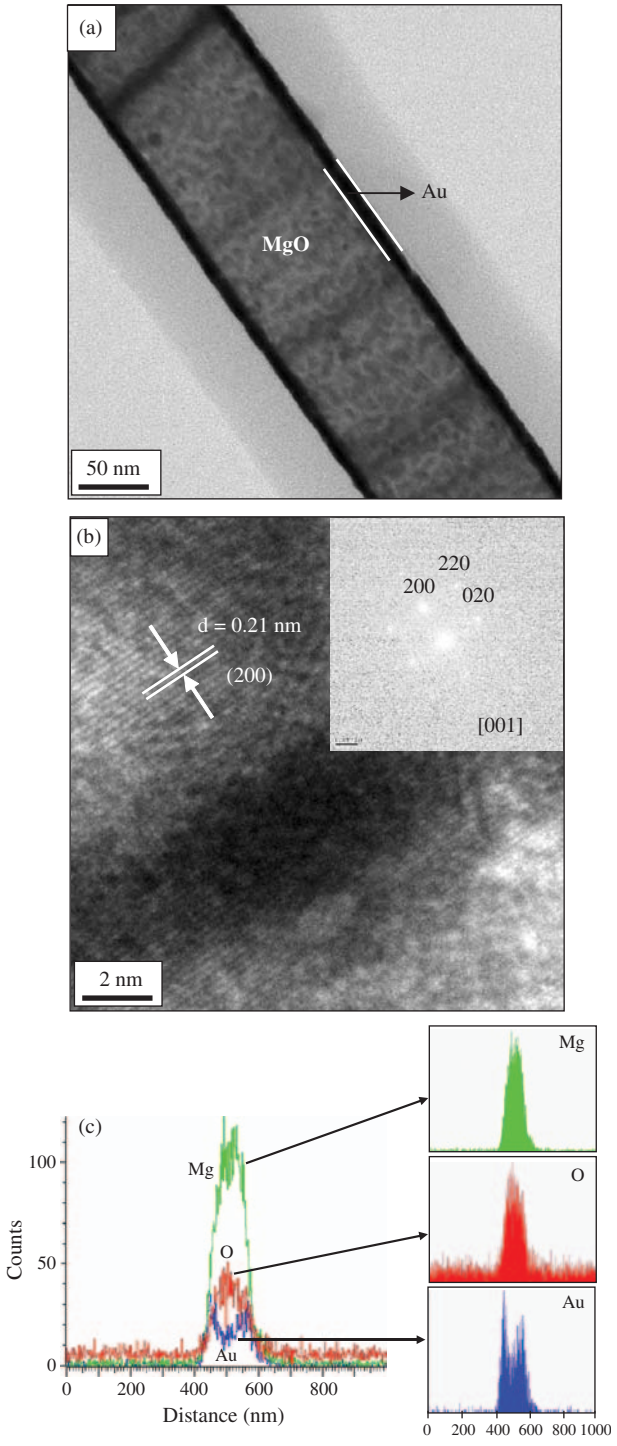

Fig. 3. (a) TEM image of a MgO nanowire coated with a continuous Au shell layer. (b) HRTEM image taken from a central region of the coated nanowire shown in (a) (inset: corresponding SAED pattern). (c) EDX line profiles of Mg, O, and Au, respectively, across the MgO/Au core–shell nanowire.

Comparison of Figure 2(c) with Figure 2(b) reveals that the relative intensities of Au-associated peaks to those of MgO-related peaks are increased with increasing sputter time, presumably due to thickening of the Au shell layer.

Figure 3(a) shows a TEM image of a coated MgO nanowire, with an Au sputtering time of 1 min. The nanostructure is indeed a nanowire having a dark outerlayer with a thickness in the range of 10–12 nm. Figure 3(b) shows a lattice-resolved high resolution TEM (HRTEM) image taken from the central part of the nanowire shown in Figure 3(a). The interplanar spacing is about 0.21 nm, corresponding to the {200} planes of cubic MgO. The associated selected area electron diffraction (SAED) pattern along the [001] axis is shown in the inset of Figure 3(b). The SAED pattern can be indexed (their hkl indices are given in the inset) according to their cubic MgO structure, revealing the single-crystalline nature of the core MgO nanowires. We surmise that a sufficiently thin Au shell layer does not influence the HRTEM image and SAED pattern of the core MgO nanowire. Figure 3(c) shows the EDX line profiles of Mg, O, and Au, respectively, across the diameter of a coaxial nanowire, confirming the existence of Mg, O, and Au elements with a rather uniform intensity profile for Mg and O, and a valley-like profile for Au. Accordingly, EDX line profiles and the TEM image are in good agreement with the predicted profiles for the Au-shelled MgO nanowires.

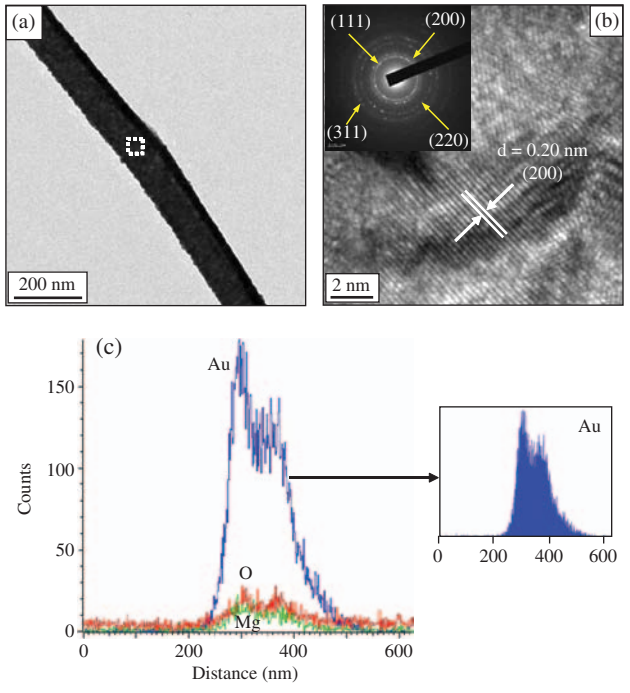

Fig. 4. (a) TEM image of a segment of a nanostructure, where a MgO core nanowire was coated with an Au layer and subsequently dipped into aqueous $(NH_3)_2SO_4$ solution. (b) HRTEM image of Au shell layer, taken at the area enclosed by the square box in (a). The inset shows the associated SAED pattern. (c) EDX line profiles of Mg, O, and Au across the diameter in a $(NH_3)_2SO_4$-dipped nanostructure.

RESEARCH ARTICLE

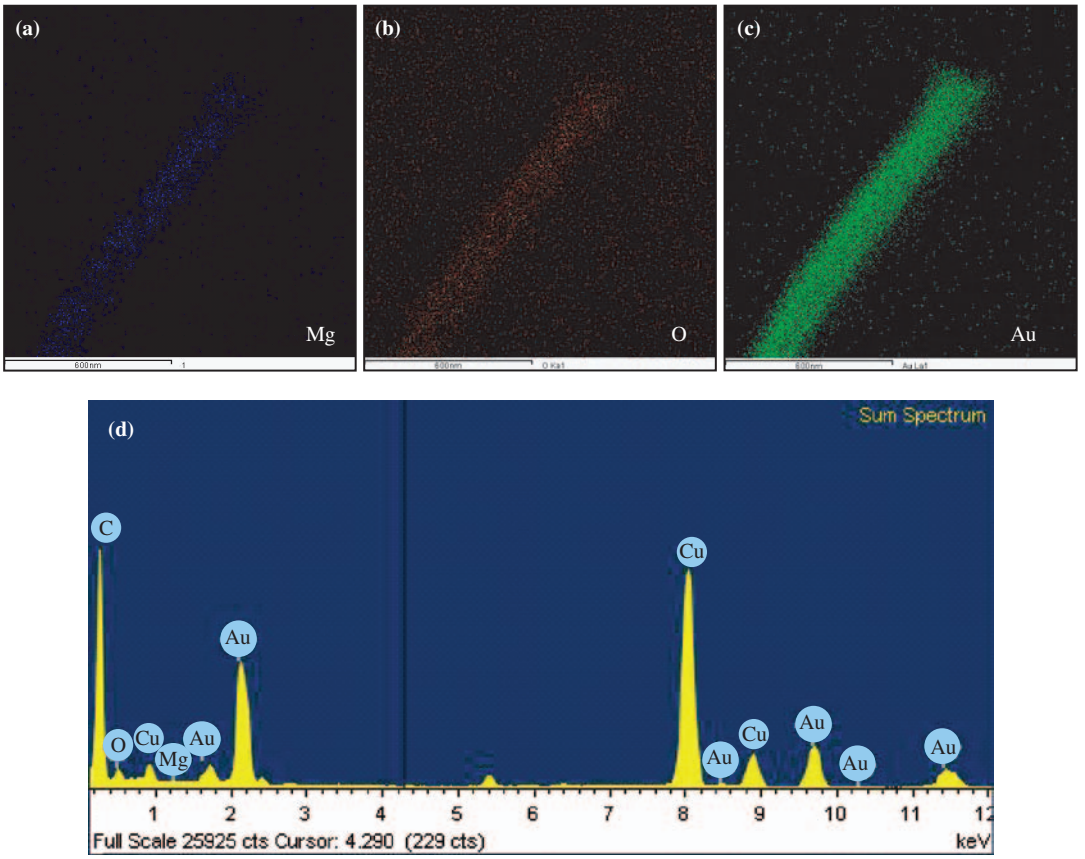

Fig. 5. EDX elemental maps of (a) Mg, (b) O, and (c) Au, respectively, from a $(NH_3)_2SO_4$-dipped nanostructure, which corresponds to an Au nanotube. (d) EDX spectrum taken from an Au nanotube.

Figure 4(a) shows a TEM image of a nanostructure obtained after coating the MgO core nanowire with an Au layer and subsequently dipping it into aqueous $(NH_3)_2SO_4$ solution. In this case, the MgO core nanowire was sputtered for 3 min. Figure 4(b) shows a lattice-resolved TEM image enlarging the area enclosed by a square box in Figure 4(a). The observed interplanar spacing is about 0.20 nm, and can be ascribed to the (200) plane of cubic Au. The lattice-resolved TEM image reveals that the shell layer comprises a crystalline phase. The inset of Figure 4(b) shows the associated SAED pattern. From the SAED analysis, diffraction rings corresponding to the (111), (200), (220), and (311) planes of the cubic Au phase were detected in the pattern, indicating that the crystal structure of the Au shell layer is polycrystalline. With the MgO core nanowires having been mostly removed, the relatively thick Au shell layer in this particular nanostructure exhibits a cubic Au phase. Figure 4(c) shows the EDX line profiles of Mg, O, and Au, respectively, along the line drawing across the diameter of a $(NH_3)_2SO_4$-dipped nanostructure. Note that Au concentrates at the shell region, whereas the Mg and O signals are significantly reduced by etching. Figures 5(a), (b), and (c) correspond to the EDX elemental maps of Mg, O, and Au, respectively, from a typical $(NH_3)_2SO_4$-dipped nanostructure. With the bright points indicating high concentrations of elements, it is revealed that the Au nanotube is of high purity. A typical EDX spectrum taken from an Au nanotube indicates that the coated nanowire mainly consists of Au elements; the presence of C and Cu peaks can be attributed to the supporting C-coated Cu grid used for the TEM analysis (Fig. 5(d)). Only trace amounts of Mg and O have been found, in agreement with the line profiles and elemental maps. Based on the HRTEM, SAED, and EDX analyses, the experimental results demonstrate that hollow Au nanotubes were successfully synthesized using MgO nanowires as sacrificial cores in tandem with an Au sputter deposition technique. The inner diameters of the Au nanotubes are determined by the diameters of the MgO core nanowires, whereas the thickness of the outer Au nanoshell can be adjusted by varying the sputtering conditions. Further study is in progress for improving the purity of the Au nanotubes by tuning the dipping conditions.

4. CONCLUSION

In summary, we demonstrated a sacrificial template route for the preparation of Au nanotubes. Au shells were coated by a sputtering method. The results of TEM and EDX analyses were in good agreement with the predicted

profiles for the Au-shelled MgO nanowires. Subsequently dipping the coated nanostrucure into aqueous $(NH_3)_2SO_4$ solution yielded hollow Au nanotube-like structures, as confirmed by HRTEM images, SAED patterns, and EDX analyses. EDX analyses revealed that the as-synthesized Au nanotubes are of high purity. The method described here is expected to be extendable to other metals, by which metal nanotubes can be fabricated with appropriate controls.

Acknowledgment: This work was supported by an Inha University research grant.

References and Notes

1. T. A. Taton, C. A. Mirkin, and R. L. Letsinger, *Science* 289, 1757 **(2000)**.
2. S. R. Nicewarner-Peña, R. G. Freeman, B. D. Reiss, L. He, D. J. Peña, I. D. Walton, R. Cromer, C. D. Keating, and M. J. Natan, *Science* 294, 137 **(2001)**.
3. L. A. Dick, A. D. McFarland, C. L. Haynes, and R. P. Van Duyne, *J. Phys. Chem. B* 106, 853 **(2002)**.
4. P. M. Tessier, O. D. Velev, A. T. Kalambur, J. F. Rabolt, A. M. Lenhoff, and E. W. Kaler, *J. Am. Chem. Soc.* 122, 9554 **(2000)**.
5. S. A. Maier, M. L. Brongersma, P. G. Kik, S. Meltzer, A. A. G. Requicha, and H. A. Atwater, *Adv. Mater.* 13, 1501 **(2001)**.
6. R. C. Hayward, D. A. Saville, and I. A. Aksay, *Nature* 404, 56 **(2000)**.
7. D. Aherne, S. N. Rao, and D. Fitzmaurice, *J. Phys. Chem. B* 103, 1821 **(1999)**.
8. M. Wirtz, S. Yu, and C. R. Martin, *Analyst* 127, 871 **(2002)**.
9. M. Wirtz, M. Parker, Y. Kobayashi, and C. R. Martin, *The Chemical Record* 2, 259 **(2002)**.
10. Z. Siwy, L. Trofin, P. Kohli, L. A. Baker, C. Trautmann, and C. R. Martin, *J. Am. Chem. Soc.* 127, 5000 **(2005)**.
11. M. del Valle, C. Tejedor, and G. Cuniberti, *Phys. Rev. B* 74, 045408 **(2006)**.
12. S. K. Lee, W. Lee, M. Alexe, K. Nielsch, D. Hesse, and U. Gösele, *Appl. Phys. Lett.* 86, 152906 **(2005)**.
13. M. A. Sanchez-Castillo, C. Couto, W. B. Kim, and J. A. Dumesic, *Angew. Chem.* 116, 1160 **(2004)**.
14. G. Jágerszki, R. E. Gyurcsányi, L. Höfler, and E. Pretsch, *Nano Lett.* 7, 1609 **(2007)**.
15. Y. Oshima and A. Onga, *Phys. Rev. Lett.* 91, 205503 **(2003)**.
16. M. Wirtz and C. R. Martin, *Adv. Mater.* 15, 455 **(2003)**.
17. P. Shao, G. Ji, and P. Chen, *J. Membrane Sci.* 255, 1 **(2005)**.
18. W. Dong, H. Dong, Z. Wang, P. Zhan, Z. Yu, X. Zhao, Y. Zhu, and N. Ming, *Adv. Mater.* 18, 755 **(2006)**.
19. S. H. C. Liang and I. D. Gay, *J. Catal.* 101, 293 **(1986)**.
20. P. D. Yang and C. M. Lieber, *Science* 273, 1836 **(1996)**.
21. G. P. Summers, T. M. Wilson, B. T. Jeffries, H. T. Tohver, Y. Chen, and M. M. Abraham, *Phys. Rev. B* 27, 1283 **(1983)**.
22. H. W. Kim, N. H. Kim, J. H. Myung, and S. H. Shim, *Phys. Stat. Sol. (a)* 202, 1758 **(2005)**.

Received: 21 November 2007. Revised/Accepted: 28 November 2007.